PRODUCTION OF RADIOACTIVE NUCLEAR BEAMS AT THE ACCULINNA SET-UP

A.S. Fomichev, A.M. Rodin, S.I. Sidorchuk, S.V. Stepantsov, G.M. Ter-Akopian, R. Wolski, I. David,
M.L. Chelnokov, V.A. Gorshkov, A.Yu. Lavrentev, B.N. Gikal, G.G.Gulbekian, S.L.Bogomolov,
V.B. Kutner, A.N.Lebedev, and Yu.Ts. Oganessian

Flerov Laboratory of Nuclear Reactions, JINR, Dubna, 141980 Russia

The primary beams of ^{7}Li, ^{11}B, ^{13}C, ^{15}N and ^{18}O ions with energies 32, 34, 43, 47 and 36 MeV/amu, respectively, delivered by cyclotron U-400M were used for producing secondary radioactive nuclear beams (RNB) at the ACCULINNA set-up. The best results were obtained with the use of Be production targets, though hydrogen and deuterium targets were tested also. Beams of ^{6,8}He, ^{11}Li, ^{12}Be and ^{8}B ions with intensities of $1.1 \cdot 10^{6}$, $2.7 \cdot 10^{3}$, $2.6 \cdot 10^{2}$, $1.3 \cdot 10^{4}$ and $4.3 \cdot 10^{3}$, respectively, were obtained.

1. Introduction

Secondary beams of radioactive nuclei (RNB), obtained with the use of intermediate energy primary beams of heavy ions were used extensively to investigate the structure of light halo nuclei. Mostly, the measurements of nuclear matter radii and momentum distributions of fragmentation reaction products were carried out at the RNB energy >40 MeV/amu to extract information about halo nuclei (see e.g. Ref. [1]). Evidently, transfer reactions involving radioactive beams can provide new information on the structure of halo nuclei complementary to the one obtained from the break-up reactions. These reactions will even allow an access to the investigation of the role of different configurations predicted by theory for these nuclei (see e.g. Ref. [2]). Transfer reactions with the beams of stable nuclei were used very effectively for the spectroscopic study of neutron-rich light nuclei [3]. However, their use with RNB was restricted so far to one case when the unbound state of ^{10}He was investigated with the use of one-neutron transfer ^{11}Li+^{2}H→^{10}He+X [4]. Also, rather restricted was the study of charge-exchange reactions using radioactive beams where one can extract information on the mechanism of heavy ion charge exchange and the Gamov-Teller Fermi transition strengths between the nuclear states (see e.g. Ref. [5]).

Radioactive ions are suitable for the transfer reaction study due to their low reaction Q-values typical for the case when new exotic nuclear systems are obtained in the reaction exit channel. This results in enhanced production cross sections for these exotic systems. Another reason why the cross sections could be large is that one can reach the new exotic nuclei of interest using one- and two-nucleon transfers or transfers of relatively stable clusters (^{4}He, ^{3}He, ^{3}H, etc.). It is known that in terms of the cross section value such transfers are more preferable than multi-nucleon transfer reactions involving the beams of stable nuclei (see e.g. Ref. [3]).

At the energy E/A≤40 MeV/amu, below the nuclear Fermi energy, the relative motion of outermost nucleons and their motion around a heavy core (a typical situation encountered in halo nuclei) strongly affect the reaction dynamics. The energy range of 15−30 MeV/amu is especially interesting because the transfer reaction cross sections still are high enough, whereas, due to the short interaction time, single-step transfers, which are more transparent for theory interpretations, are more probable as compared to the multi-step ones. Estimations based on the empirical systematic [3] show that the cross sections of the relevant reactions will be $10^{-27}-10^{-30}$ cm^{2}/sr. When halo (drip-line) nuclei are involved in transfer reactions, typical is the situation that both exit channel products do not have particle stable excited states. Therefore a RNB energy spread of 3-5 % appears to be tolerable for such experiments. One can hardly reduce the energy spread assuming that the intensity of a secondary beam is important for experiments. One should measure transfer reaction differential cross sections with a good angular resolution. This requires that the RNB angular divergence should be limited to a relatively small value. For light, A=1−8 targets a maximum beam divergence angle of 1° (≈17 mr) will be tolerable for the most cases.

The ACCULINNA set-up [6-8] is suitable for the generation of secondary radioactive beams in this energy range due to the primary heavy ion beams of high intensity accessible from the U-400M cyclotron. An attractive point is that the heavy ion energy of 30−50 MeV/amu, which one can easily set at the cyclotron, is convenient for producing the secondary beams having an energy of 15−30 MeV/amu. Also, the variety of beams ranging from ^{7}Li to ^{18}O, delivered by the cyclotron, facilitates the observation of optimum conditions for obtaining the beams of exotic nuclei with Z≤8. In the following two sections the ACCULINNA set-up is briefly described, and production of primary beams of the U-400M cyclotron is outlined. Experiments and results obtained on the RNB production are described in the last section.

2. Description of ACCULINNA

The layout of ACCULINNA is shown in fig.1. The beam line originates from the dipole magnet D0 turning the cyclotron primary beam to the object plane F1 of the line. Quadrupole doublet Q01-Q02 working in accord with the preceding magnetic elements provides the focus of the primary beam on the main object slit, where the production target is placed. The main beam line of ACCULINNA involves two 30-degree sector dipole magnets (D1, D2) and four doublets of quadrupole lenses (Q1-Q8). For

minimizing aberrations in focal planes F2 and F3, magnetic sextupole lenses SX1 and SX2 are installed in the drift spaces between lenses Q3, Q4 and Q7, Q8, respectively. The maximum magnetic rigidity of the beam line in the achromatic mode makes 3.6 Tm. The line transfers RNB to the physics target positioned in the main focal plane F3 of the beam line.

In the achromatic mode ACCULINNA has an intermediate focus in its symmetry plane F2 where a wedge-shaped degrader is installed for the elimination of RNB impurities. Two different options for the tuning of the ACCULINNA beam line result in the capture of exotic nuclei emerging from the production target within a solid angle of 0.3 msr and 0.7 msr, respectively. For both options, the momentum dispersion is 5.6 mm/% in plane F2, and secondary beams having a momentum spread of (maximum) ±3% are transmitted to the physics target. If the degrader profile is chosen to preserve the achromatic image, the object magnification in F3 is 1 and 1.5, respectively, for the two ACCULINNA tuning modes. Dispersion in focal plane F3, related to the energy loss in the degrader, is 11 mm/%. Reduction of the RNB energy spread can be achieved in two ways: a) by decreasing the slit dimension in focal plane F2, b) by using another degrader profile allowing to reduce the RNB momentum spread to $3 \cdot 10^{-3}$ at the expense of increasing the beam transverse phase space. In the present study we used the first way and worked mostly with a slit eliminating the RNB maximum momentum spread to ±2.1 %.
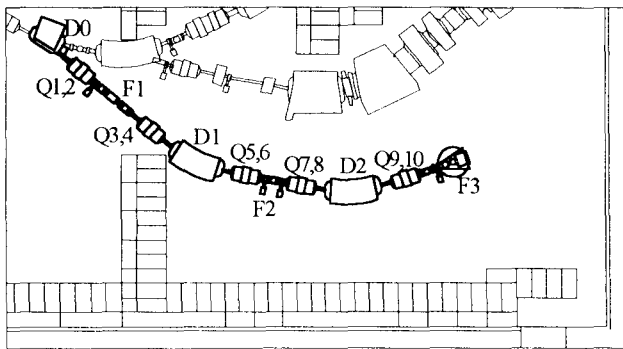

Figure 1 : ACCULINNA layout.

Focal plane F3 is located inside a reaction chamber intended for housing the physics target and detector arrays. The chamber contains two arms providing the independent rotation of two ΔE–E particle telescopes. Telescopes employed for monitoring RNB involved silicon strip detectors (detector area 58×58 mm^2, thickness – 300 μ number of strips – 29, strip width – 2 mm), surface-barrier Si detectors (65 mm in diameter and 0.5–0.6 mm thick) and a thick Si-Li detector (66 mm in diameter and 7.7 mm thick). Two strip detectors were used in one telescope for measuring x and y coordinates of each incoming ion. Specific energy losses were measured either by the strip and surface-barrier detectors or by the strip detectors only. In some cases a thick (15 mm) CsI(Tl) crystal viewed by a photo-multiplier was used to measure the rest energy of ions. The energy resolution of all the Si detectors was about

100 keV for 5.5 MeV α-particles and made 0.6% for 155 MeV ^{4}He ions. An energy resolution of ≈1 % was obtained for 150 MeV ^{6}He ions with the CsI(Tl) spectrometer. A maximum count rate of 10^3 ions/s was allowed for the telescopes. Higher count rates, up to 3×10^5 s^{-1}, were monitored by a single thin (150 μm NE PILOT-U) ΔE plastic scintillation detector.

Both solid matter and gaseous materials were tested as RNB production targets. A gaseous hydrogen target (a gas cell working at a pressure of up to 50 atm) was used in our experiments for the first time. The gas cell was cooled by water; it had a length of 10 cm along the beam direction and 100 μm stainless steel entrance and exit windows of a diameter of 10 mm.

The ACCULINNA beam line was tested using a primary beam of 151 MeV/amu ^{14}N ions. About 70% of the ^{14}N beam coming from the U-400M cyclotron were focused onto the main object slit of the size of 3×10 mm^2. In experiments on the production of RNB a diaphragm of 6 mm in diameter was installed in front of the solid material target. Two diaphragms provided the focusing of the primary beam in a 5 mm spot in the symmetry plane of the hydrogen target.

3. Primary beams

Since 1995 the heavy ion cyclotron U-400M operates with an ECR ion source DECRIS-14 (Dubna ECR Ion Source). In order to inject an ion beam from the source into the acceleration area a system of the axial injection was created. Main parameters of the U-400M cyclotron are presented in the Table 1.

Table 1 : Characteristics of U-400M cyclotron.

Pole diameter (m)	4
Average magnetic field (T)	1.5-1.9
Number of dees	4
Dee voltage (V)	1500
RF frequency (MHz)	11.5-24.5
A/Z range	2-5
Ion energies (MeV/amu)	25-100
Beam extraction	charge exchange

A number of primary beams suitable for the production of light RNB were accelerated and transported to the production target of ACCULINNA: ^{7}Li (32 MeV/amu), ^{11}B (34 MeV/amu, ^{13}C (43 MeV/amu), ^{15}N (47 MeV/amu) and ^{18}O (36 MeV/amu). The energy spread of the beam extracted from the cyclotron made about 1%. As an example, the beam current (in pps) of ^{7}Li ions on different stages of acceleration is presented in the Table 2.

Table 2 : Beam intensities of ^{7}Li ions at different acceleration stages.

Injection	^{7}Li^{+2}	$2.7 \cdot 10^{14}$
R=20 cm	^{7}Li^{+2}	$1 \cdot 10^{13}$
Extraction radius R=161 cm	^{7}Li^{+2}	$9 \cdot 10^{12}$
Beam line	^{7}Li^{+3}	$2 \cdot 10^{12}$
Physics target (F3)	^{7}Li^{+3}	$2 \cdot 10^{12}$

Presently, the efficiency of the beam extraction from the cyclotron is increased to 80 %. 70 % of ions, accelerated to the beam extraction orbit, are delivered to the 6 mm diaphragm of the production target where beam intensities of 3.5 and 6.0 eμA of ^{11}B and ^{13}C, respectively, were obtained in long term target irradiation.

A serious problem is a steady and long-term operation of DECRIS-14 when ^{7}Li ions are accelerated. Lithium vapour comes into the ion-source discharge chamber from a micro-oven where a lithium metallic sample is heated and evaporated. The oven consists of the stainless steel body, ceramic insulators and a heater (NiCr wire) contained in a stainless steel tube. A power of only a few watts is required in order to reach the temperature of the work mode of the evaporation. Helium as a support gas is used in the ion source. The time of a steady work of the oven makes about 300 hours. A hot metallic screen that is maintained at a temperature of $\approx 400°C$ prevents the absorption of lithium on the walls of the chamber. Some results for the yields of ions from DECRIS-14 obtained during our experiments are presented in Table 3.

Table 3 : Yields (eμA) from DECRIS-14.

Q	+1	+2	+3	+4
^{7}Li	180	290	50	
^{11}B	20	55	100	50
^{13}C		38	38	48

4. Secondary beams

The primary beams of ^{7}Li, ^{11}B, ^{13}C, ^{15}N and ^{18}O from the cyclotron U-400M were used for the production of a number of secondary RNB. Several types of the production target were examined for the RNB production. The first one is the hydrogen gaseous production target operated at the work pressure 30 atm. The thickness of the hydrogen target made $1.4 \cdot 10^{22}$ cm^{-2}. The solid targets used are listed in Table 4.

Table 4 : Parameters of production targets.

Target	Thickness (mg/cm^2)
Polyethylene (C$_2$H$_4$)$_n$	19
Heavy polyethylene (C$_2$D$_4$)$_n$	22
Graphite	36
Beryllium	175 - 680
Tantalum	165 - 330

In order to find the optimum tunings of the spectrometer the dependence of the yield of the specific RNB on its magnetic rigidity was measured at each projectile-target combination. The measurements were performed in the achromatic mode of the spectrometer. Achromatic aluminium wedges (with a thickness of 210 and 350 mg/cm^2 along the beam axis) were used in these experiments. To monitor the primary beam intensity we measured the secondary electron emission current from a

6.6-mg/cm^2 tantalum foil installed just after the production target. Full aperture (58×58 mm^2) ΔE-E detector telescopes were used to detect RNB in focal plane F3. A typical ΔE-E beam matrix obtained when ACCULINNA was tuned to the optimum production of ^{8}He ions is shown in Fig.2 (reaction ^{18}O + ^{9}Be (350 mg/cm^2), wedge - 210 mg/cm^2).
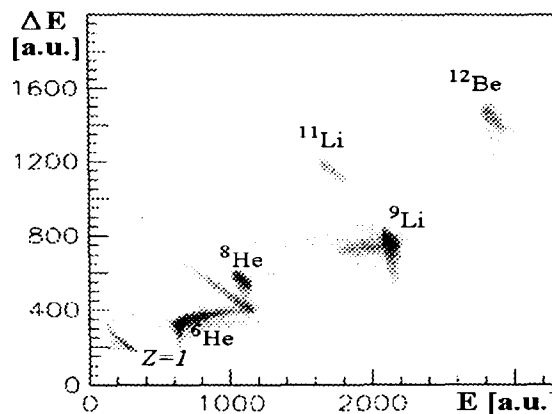
Figure 2 : ΔE-E beam matrix (see text).

The energy spread of the peak of ^{8}He makes about 7% (FWHM) and corresponds to the momentum acceptance of the beam line. The dependence of the yields of some exotic nuclei on their energy for the same projectile-target combination is shown in Fig. 3. The yield values are normalized to a beam current of 1 pμA. In reality, these measurements were
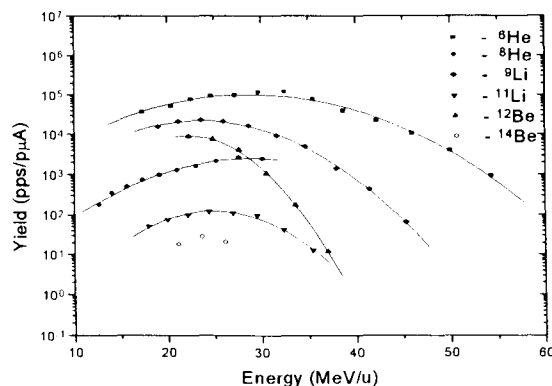
Figure 3 : Yields of exotic nuclei in function of their energy for the reaction ^{18}O + ^{9}Be (350 mg/cm^2).

carried out mostly with the primary beam current ranging from 10 to 250 enA. It is seen from Fig. 3 that the smooth dependence of the yields on the energy provides the possibility to vary the energy of RNB in a wide range without noticeable losses in the intensity.

The image of the secondary RNB in the achromatic focal plane F3 (reaction ^{18}O + ^{9}Be), at the tuning of the beam line to ^{8}He, is shown in Fig.4. The diameter of the spot corresponding to ^{8}He was found to be about 10 mm

(FWHM). It is clearly seen that the beam of ^{8}He ions is focused onto the centre of the achromatic focal plane and its size is consistent with the diameter of the main object slit. The wedge provides a satisfactory separation of different RNB in achromatic focal plane. The purity of the ^{8}He beam in the central 10 mm spot is ≈80%.

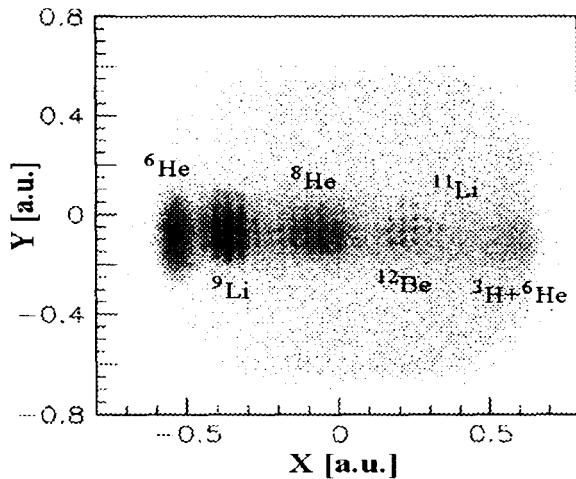| ^{8}He (33)	$2.5 \cdot 10^3 / 2.0 \cdot 10^3$	^{15}N+Be (47)
^{8}He (24)	$2.5 \cdot 10^3 / 1.1 \cdot 10^3$	^{18}O+Be (36)
^{9}Li (34)	$2.1 \cdot 10^4 / 5.8 \cdot 10^4$	^{15}N+Be (47)
^{9}Li (36)	$3.0 \cdot 10^4 / 1.0 \cdot 10^5$	^{13}C+Be (43)
^{9}Li (29)	$2.1 \cdot 10^4 / 2.5 \cdot 10^4$	^{18}O+Be (36)
^{11}Li (35)	$2.6 \cdot 10^2 / 1.3 \cdot 10^2$	^{15}N+Be (47)
^{11}Li (27)	$1.3 \cdot 10^2 / 1.0 \cdot 10^2$	^{18}O+Be (36)
^{12}Be (27)	$5.3 \cdot 10^3 / 1.3 \cdot 10^4$	^{15}N+Be (47)
^{12}Be (27)	$1.3 \cdot 10^4 / 9.3 \cdot 10^3$	^{18}O+Be (36)
^{14}Be (26)	$4.0 \cdot 10^1 / 4.1 \cdot 10^1$	^{18}O+Be (36)
^{15}B (23)	$2.4 \cdot 10^3 / 9.0 \cdot 10^3$	^{18}O+Be (36)
^{8}B (38)	$4.3 \cdot 10^3 / 1.5 \cdot 10^4$	^{15}N+Be (47)

Figure 4 : The beam profile in the achromatic focal plane F3 (^{18}O + ^{9}Be reaction, the ^{8}He tune).

Maximum yields of ^{6}He ions obtained in reactions of 32 MeV/amu ^{7}Li ions are shown in Table 5. The yields for hydrogen and deuterium in polyethylene targets have been obtained after subtraction of the background due to the carbon in polyethylene. The data are normalized to the value of primary beam current of 1 pµA and the thickness of a hydrogen (deuterium) target of $1 \cdot 10^{22}$ cm^{-2}.

Table 5 : Yield of ^{6}He in the reactions of ^{7}Li ions with hydrogen and deuterium.

Target	Y_{max} (pps/pµA)	Wedge (mg/cm^2)
H (gas)	$6.7 \cdot 10^3$	0
H (C_2H_4)	$3.3 \cdot 10^3$	630
D (C_2D_4)	$1.3 \cdot 10^4$	630

The maximum yields of some exotic nuclei produced with different projectiles on the beryllium target are presented in Table 6. The experimental values are normalized to the primary beam current of 1 pµA and are compared with calculations made with the use of the programme LISE.

Table 6 : Maximum rates of exotic nuclei.

RNB (E, MeV/amu)	Yield, pps/pµA, exp./calc.	Reaction (E_p, MeV/amu)
^{6}He (25)	$1.1 \cdot 10^6 / 3.3 \cdot 10^5$	^{7}Li+Be (32)
^{6}He (25)	$2.7 \cdot 10^5 / 2.8 \cdot 10^5$	^{13}C+Be (43)
^{6}He (32)	$5.2 \cdot 10^4 / 1.8 \cdot 10^5$	^{15}N+Be (47)
^{6}He (30)	$1.2 \cdot 10^5 / 4.3 \cdot 10^4$	^{18}O+Be (36)
^{8}He (28)	$5.9 \times 10^3 / 5.3 \times 10^3$	^{11}B+Be (34)
^{8}He (25)	$2.4 \cdot 10^3 / 3.9 \cdot 10^3$	^{13}C+Be (43)

In experiments employing secondary beams of ^{6}He and ^{8}He, collimators eliminating the beam halo were positioned in front of a helium gas target installed in focal plane F3. These collimators limited the diameter of the beam spot on the target to 5 and 8 mm, respectively, for ^{6}He and ^{8}He. The beam currents on the target were reduced with the collimators to 30 and 40 %, respectively. The use of such a collimator reduced the energy spread and angular divergence of secondary beams. In case of ^{6}He the full width of the beam energy distribution at the half of the maximum was 2.5 %.

References

1. I. Tanihata, J.Phys. G: Nucl. Part. Phys., **22** (1996) 157.
2. V. Zhukov atal., Phys. Rep. **231** (1993) 151.
3. H.G. Bohlen et al., Low Energy Nuclear Dynamics, *XV Nucl. Phys. Divisional Conference, St. Petersburg, Russia, April, 1995*. Yu. Oganessian, R. Kolpakchieva and W. Von Oertzen (Eds.), World Scientific, Singapore, 1995, p. 53.
4. A.A. Korsheninnikov et al., Phys. Lett. **B326** (1994) 31.
5. B.M. Sherrill et al., Nucl. Phys. **A616** (1996) 145c.
6. A.M. Rodin et al., Nucl. Insr. & Meth. In Phys. Res. **A391** (1997) 228.
7. A.M. Rodin at al., Nucl. Insr. & Meth. In Phys. Res. **B126** (1997) 236.
8. A.M. Rodin et al., Nucl. Phys. **A626** (1997) 567c.